Polymer International

Polym Int 56:1340–1348 (2007)

Engineering electrospun nanofibrillar surfaces for spinal cord repair: a discussion

Sally Meiners,[1]* Ijaz Ahmed,[1] Abdul S Ponery,[1] Nathan Amor,[1] Suzan L Harris,[1] Virginia Ayres,[2] Yuan Fan,[2] Qian Chen,[2] Roberto Delgado-Rivera[1,3] and Ashwin N Babu[1]

[1]*Department of Pharmacology, UMDNJ-Robert Wood Johnson Medical School, Piscataway, NJ 08854, USA*
[2]*Department of Electrical and Computer Engineering, Michigan State University, East Lansing, MI 48824, USA*
[3]*Department of Chemistry and Chemical Biology, Rutgers University, Piscataway, NJ 08854, USA*

Abstract

BACKGROUND: The design of implants comprised of biodegradable electrospun nanofibers for the purpose of bridging injuries in damaged spinal cord is discussed. Electrospun nanofibers structurally mimic the extracellular matrix on which neurons and other cell types grow *in vivo*. This property has created great interest for their use in tissue engineering applications. However, their employment as biomimetic surfaces for such *in vivo* applications is still in its infancy.

RESULTS: A nonwoven fabric comprised of electrospun polyamide nanofibers supported modest axonal regeneration in injured adult rat spinal cord. Covalent modification of the nanofibers with a bioactive peptide derived from the neuroregulatory extracellular matrix molecule tenascin-C enhanced the ability of the nanofibers to facilitate axonal regrowth. However, the random orientation of the nanofibrillar fabric folds was an impediment to the forward movement of axons.

CONCLUSIONS: Polyamide nanofibers covalently modified with neuroactive molecules provide a promising material for grafts to promote spinal cord regeneration. However, for the proper guidance of regrowing axons, attention must be paid to the engineering of ordered nanofibrillar structures.

Keywords: nanofiber; neuron; tenascin-C; peptide; extracellular matrix; spinal cord

INTRODUCTION

During development of and following injury to the nervous system, the growth and regeneration of axons is strongly influenced by astrocyte-derived extracellular matrix molecules[1] and Schwann cell-derived basement membrane molecules.[2] (The basement membrane is a structurally compact form of the extracellular matrix.) Examples of such molecules include thrombospondin in the extracellular matrix[3] and laminin-1 in the basement membrane.[4] Therefore, artificial scaffolds that are extracellular matrix/basement membrane-mimetic might provide ideal substrates for neuronal growth, particularly for *in vivo* applications that require regenerative scaffolds to be compatible with tissue. Although the extracellular matrix produced by astrocytes includes both positive (e.g. thrombospondin, fibronectin) and negative (e.g. chondroitin and keratan sulfate proteoglycans) effectors of neuronal growth,[1,4–6] the underlying hypothesis is that nanofibers will form a scaffold that mimics extracellular matrix-based supportive as opposed to inhibitory cues.

Work with electrospun nanofibers has supported this hypothesis.[7] Nanofibers produced via the process of electrospinning have unprecedented porosity, a high surface to volume ratio and high interconnectivity, all physical properties that are ideal for cellular attachment and growth.[7] The nanofiber aggregates can be deposited in either a random or aligned array, to result in random or oriented axonal growth.[8] Moreover, the geometry of the nanofibers mimics the fibrillar organization of the extracellular matrix that forms a network for neuronal attachment and axonal growth during central nervous system (CNS) development. Nanofibers electrospun from a variety of synthetic and naturally occurring polymers have thus

* Correspondence to: Sally Meiners, Department of Pharmacology, UMDNJ-Robert Wood Johnson Medical School, 675 Hoes Lane, Piscataway, NJ 08854, USA
E-mail: meiners@umdnj.edu
Contract/grant sponsor: National Institutes of Health; contract/grant number: R01 NS40394
(Received 2 March 2007; revised version received 17 July 2007; accepted 23 July 2007)
Published online 13 September 2007; DOI: 10.1002/pi.2383

 Polym Int 0959–8103/2007/$30.00

06-3058

generated tremendous interest due to their potential as scaffolds for regenerating tissue,[9–12] with a recent study indicating that silk nanofibers improved bone regeneration in the rabbit.[13]

Chemistry as well as geometry of the extracellular matrix is critical for proper neuronal function, necessitating that an optimized biomimetic surface for CNS repair incorporate both types of cues. Tenascin-C, a multidomain, multifunctional extracellular matrix glycoprotein with neuroregulatory actions,[14–18] provides an example of a chemical cue that might enhance the function of a nanofibrillar scaffold. The alternatively spliced fibronectin type III region of human tenascin-C has demonstrated growth-promoting actions for a variety of neuronal types.[14,16] The active site for neurite outgrowth in this region from cerebellar granule, cerebral cortical, spinal cord motor and dorsal root ganglion neurons was localized to a peptide with amino acid sequence VFDNFVLKIRDTKK,[18,19] called the D5 peptide. Covalent modification of electrospun polyamide nanofibers with the D5 peptide promoted more *in vivo*-like growth patterns for neurons, with long, well-elaborated processes.[19] This in turn suggests that the peptide-modified nanofibers may find therapeutic applications in the repair of spinal cord injury and other CNS disorders.

Despite interest in using nanofibers in applications for spinal cord repair,[8] there has been little discussion about how this might actually be accomplished. Therefore, we turned our attention to this question. Given our initial success with the use of polyamide nanofibers as modifiable scaffolds for the growth of neurons *in vitro*, the hypothesis was explored that polyamide nanofibrillar matrices, alone or derivatized with the D5 peptide, can serve as biomimetic, regenerative implants following injury to the spinal cord.

EXPERIMENTAL

Polyamide nanofibers

Randomly oriented polyamide nanofibers (continuous fibers that collect as a nonwoven fabric) were electrospun by Donaldson Co., Inc. (Minneapolis, MN). They were electrospun from a blend of two polymers, $(C_{28}O_4N_4H_{47})_n$ and $(C_{27}O_{4.4}N_4H_{50})_n$, either onto plastic (Aclar) coverslips for imaging studies or as a free fabric for spinal cord studies. The polymeric nanofiber mat was crosslinked in the presence of an acid catalyst and formed a network of filaments on average 180 nm in diameter interspersed with pores 100–800 nm in diameter.[20] In some cases the nanofibers were covalently coated with a proprietary polyamine polymer by Surmodics, Inc. (Eden Prairie, MN) to provide functional groups for further covalent modification of the nanofibers with bioactive peptides.

Nanofibers for the spinal cord studies were either unmodified or covalently modified with a neurite outgrowth-promoting peptide derived from tenascin-C, called the D5′ peptide. (The complete covalent modification method is described in Ahmed *et al.*[19]) The amino acid sequence of the D5′ peptide is ADEGVFDNFVLKIRDTKKQ, where FD and FV are required for facilitation of neurite extension.[18]

Atomic force microscopy

Nanofibers (unmodified and peptide-modified) for the imaging studies were visualized using AFM as follows. Contact mode, friction force and tapping mode AFM were performed in ambient air using a Nanoscope IIIa MulitMode system from Veeco Instruments, Inc (Woodbury, NY). A J-scanner with a maximum $125 \times 125\,\mu m^2$ x–y scan range was used, with 512×512 pixels recorded for each image. Silicon nitride tips with a nominal 20–25 nm tip radius of curvature were used for contact mode AFM, and etched silicon tips with a nominal 5–10 nm tip radius of curvature were used for tapping mode AFM. On each sample, a series of corresponding 100, 25 and $10\,\mu m^2$ areas were examined in contact mode AFM. On each sample a further series of corresponding 10, 5 and *ca* $2.5\,\mu m^2$ areas were examined in tapping mode AFM.

Surgical procedure and postoperative care

To investigate whether polyamide nanofibers allow axonal regrowth *in vivo* following CNS injury, unmodified or peptide-modified nanofibers were incorporated into an over-hemisection spinal cord injury model. The subjects of this study included 5 animals with unmodified nanofibrillar implants, 5 animals with peptide-modified nanofibrillar implants and 5 injury-only control animals for the visualization of axons (3 weeks survival time); and 10 animals with unmodified nanofibrillar implants and 10 injury-only control animals for the visualization of cell bodies (3 and 5 weeks survival time; 5 animals for each group and each time point).

Adult female Sprague Dawley rats (250–260 g) were anesthetized using ketamine/xylazine ($75\,mg\,kg^{-1}$ + $10\,mg\,kg^{-1}$, intraperitoneal (IP)). They were also given buprenorphine ($0.05\,mg\,kg^{-1}$, delivered subcutaneously) on a pre-emptive basis for postoperative pain. A laminectomy was made at the thoracic level 8 (T_8) spinal vertebrae. Iridectomy scissors were stereotaxically positioned at the dorsal midline of the spine and lowered to a depth of 2.0 mm. A piece of polyamide nanofiber fabric (*ca* $5 \times 5\,mm^2$) comprised of randomly deposited fibers with a thickness of $2–4\,\mu m^2$ was gently crumpled with a pair of micro-forceps and carefully implanted into the lesion site. Control animals received no nanofibers. The 2–4 μm thickness of the fabric was chosen because thinner layers of nanofibers were very difficult to handle, while thicker layers of nanofibers lost their flexibility. The musculature

was sutured and the skin was closed with surgical clips. All animal procedures were performed in strict accordance with institutional guidelines (Institutional Animal Care and Use Committee Approval no. PI04-063-06).

Animals were allowed to recover in clean cages atop heating pads. They were observed for infection or lethargy and were treated for 4 days postsurgery with buprenorphine analgesic (0.05 mg kg^{-1}, 2–3 times daily, delivered subcutaneously). Animals were also injected subcutaneously with enrofloxacin (Baytril) antibiotic for at least 3 days to manage bladder infections (5 mg kg^{-1}, 2 times daily) and with Ringer's lactate solution (5 mL, 3 times daily, delivered subcutaneously) for 2–3 days (or until animals were observed to be drinking on their own) to manage dehydration. Bladders were evacuated 3 times daily until autonomic bladder function was restored (usually 4–7 days).

Immunohistochemistry

Following postoperative periods of 3 or 5 weeks, animals were transcardially perfused under deep terminal anesthesia (sodium pentobarbital, 100 mg kg^{-1}, IP) with 4% paraformaldehyde in 0.1 mol L^{-1} sodium phosphate buffer. Spinal cords were removed and sagittally sectioned on a cryostat at 20 µm. Sections were mounted on poly(L-lysine)-coated glass slides and stained for cell bodies using Nissl stain or immunolabeled for axons using monoclonal mouse antibody against neurofilament-M (Chemicon, Temecula, CA) (1:400 dilution overnight at room

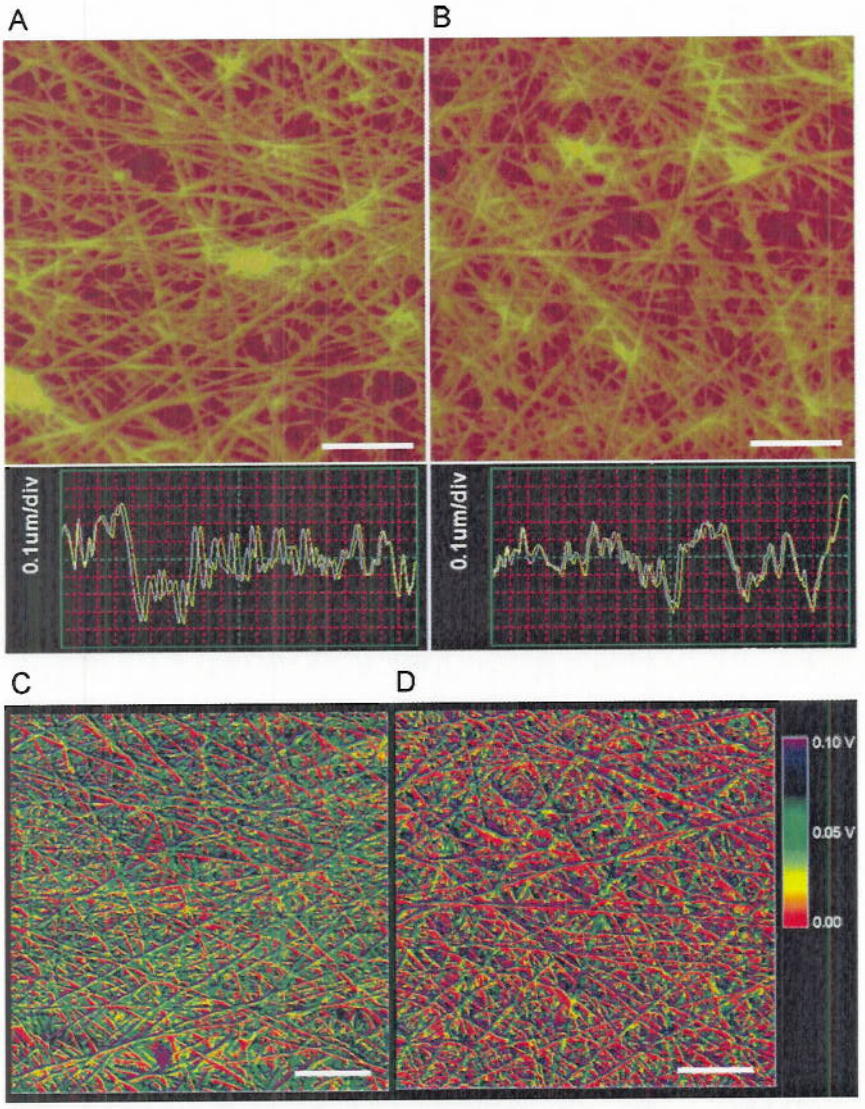

Figure 1. Network of electrospun polyamide nanofibers. Images of nanofibers electrospun onto plastic coverslips. Contact mode AFM images of (A) unmodified nanofibers and (B) peptide-modified nanofibers revealed a fibrous network of filaments interspersed with pores. Line tracking for both images indicated only minor differences in how well the tip tracked the surfaces. Scale bar, 5 µm. Friction force AFM images of (C) unmodified nanofibers and (D) peptide-modified nanofibers revealed the effect of the different surface chemistries, indicated by the increased torsioning of the cantilever as the tip moved across the peptide-modified nanofibers. Scale bar, 5 µm.

Polym Int **56**:1340–1348 (2007)
DOI: 10.1002/pi

temperature) followed by a CY3-conjugated goat anti-mouse secondary antibody (Jackson ImmunoResearch, West Grove, PA) (1:500 dilution for 1 h at room temperature). At least 30–40 sections per spinal cord were examined. Slides were examined using a Zeiss Axioplan microscope equipped with an epi-fluorescence illuminator.

RESULTS

Atomic force microscopy

For each sample, a series of corresponding 100, 25 and 10 μm^2 areas were examined in contact mode AFM. Height mode and fiction force images were both investigated.[21] Height mode AFM measures the tip–sample interaction forces normal to the sample surface and provides a representation of the surface topography through Hooke's law: $F_z = k\Delta z$. Friction force AFM measures cantilever torsion and bending forces lateral to the tip motion across the sample surface and provides a representation of the surface friction through Amonton's law: $F_{\text{friction}} = \mu F_{\text{loading}}$.

Wide-area $100 \times 100\,\mu m$ scans (not shown) were first performed to assess the uniformity of the nanofiber mesh surfaces. Both unmodified and peptide-modified nanofiber meshes were uniform over $100\,\mu m^2$ areas. A corresponding series of $25 \times 25\,\mu m^2$, then $10 \times 10\,\mu m^2$ images, taken from within the $100\,\mu m^2$ scans, were examined. The $25 \times 25\,\mu m^2$ height and friction force images are shown in Fig. 1. Trace/retrace scans included below Figs 1(A) and (B) indicated good tracking for both unmodified and peptide-modified nanofibers. Height mode AFM images of unmodified nanofibers (Fig. 1(A)) and peptide-modified nanofibers (Fig. 1(B)) revealed a fibrous network of filaments interspersed with pores. Friction force AFM images of unmodified nanofibers (Fig. 1(C)) and peptide-modified nanofibers (Fig. 1(D)) revealed the effect of the different surface chemistries, indicated by the increased torsioning of the cantilever as the tip moved across the peptide-modified nanofibers. The difference in surface friction may be due to both steric and chemical effects given that the peptide was covalently bound to the nanofiber at the N-terminus end, but was otherwise free to pivot and interact as the tip moved across the sample surface.

A further series of corresponding 10 μm^2 and 5 μm^2 areas, and a close-up image *ca* 2.5 μm^2, were examined in tapping mode AFM.[22] In tapping mode AFM, a root mean square (RMS) height mode image is taken using an oscillating tip that lightly 'taps' the surface. Lateral friction forces are greatly reduced, as x–y motion occurs while the tip is raised. Furthermore, the phase difference between the natural frequency of the oscillating cantilever and the changed frequency that develops when the tip interacts with a sample surface provides a sensitive measure of the local environment.

Tapping mode AFM images (height and phase) of the unmodified nanofibers and peptide-modified nanofibers are shown in Fig. 2. The difference in the nanofiber surfaces was most apparent in the phase images (Figs 2(B) and (D)). The roughness of the peptide-modified nanofibers (Fig. 2(D)) in comparison to that of the unmodified nanofibers (Fig. 2(B)) resulted from factors that affect the RMS oscillation of the cantilever and may be due to both topographical surface roughness and to surface chemistry. Similar effects have been observed by Karakecili *et al.*[23] for unmodified *versus* RGD-modified polycaprolactone membranes.

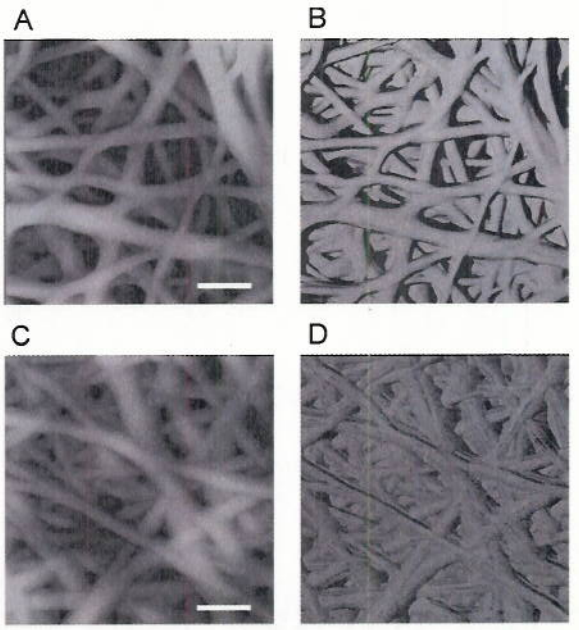

Figure 2. Close-up images of electrospun polyamide nanofibers obtained by tapping mode AFM. (A) Height image, unmodified nanofibers; (B) phase image (30°), unmodified nanofibers; (C) height image, peptide-modified nanofibers; (D) phase image (10°), peptide-modified nanofibers. The difference in the surface roughness is most apparent in the phase images. Scale bar, 1 μm.

Biocompatibility of polyamide nanofibers

To evaluate the biocompatibility of polyamide nanofibers and their potential as a regenerative matrix in injured spinal cord, a piece of nanofibrillar fabric comprised of randomly oriented nanofibers was implanted into an over-hemisection wound as described above. The fabric was well integrated into the host tissue 3 and 5 weeks after injury, with no evidence of cavitation (illustrated by Nissl staining in Fig. 3(A) for the 5 week time point), whereas a large cavity was present in injury-only, control animals (Fig. 3(B)). Imaging of sequential sections showed that the lesion site was completely filled with nanofibers. (Compare Figs 5(B), 5(C) and 6(A), all sections from the same animal.)

Axonal growth on unmodified and peptide-modified nanofibers

Axons were visualized 3 weeks after injury utilizing an antibody against neurofilament-M and epi-fluorescent

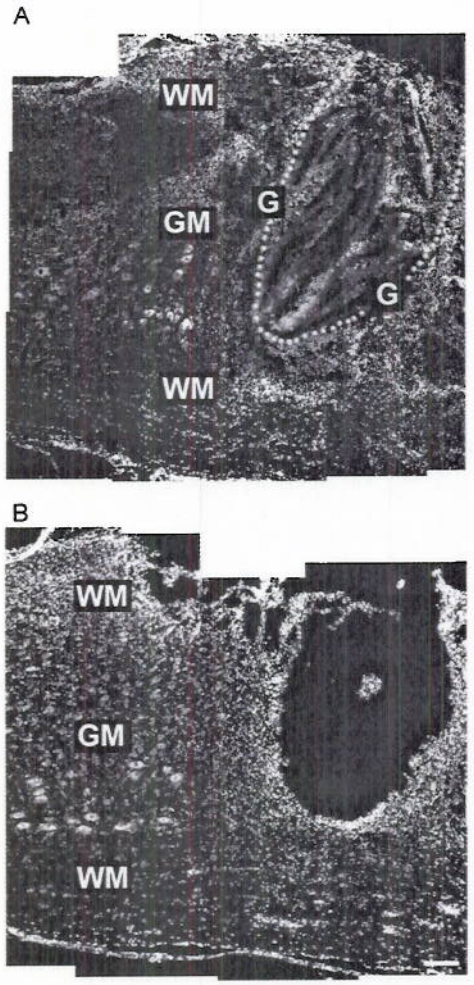

Figure 3. Nissl staining of representative spinal cord lesion site with implanted polyamide nanofibers in comparison to an injury-only control. Rostral is to the left. The implant of randomly deposited nanofibers (unmodified) (A) demonstrated good host–graft integration 5 weeks after injury with no cavitation, whereas a large cavity was present in the injury-only control (B). The area of the graft in (A) is surrounded by a dotted line. (A) and (B) each represent a montage derived from several images taken across one spinal cord section. G, host–graft interface; WM, white matter; GM, gray matter. Scale bar, 250 μm.

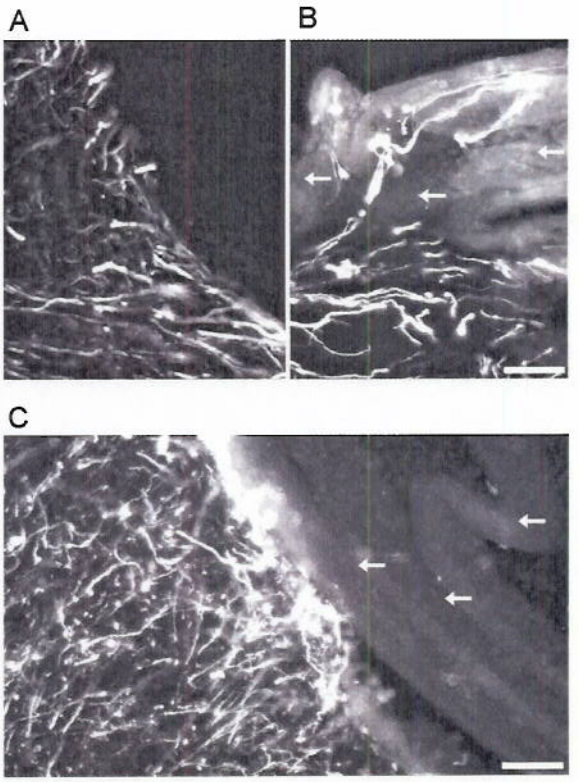

Figure 4. Neurofilament-M labeling in a representative injury-only control animal and an animal that received an unmodified nanofibrillar implant. Rostral is to the left. (A) Neurofilament-M-labeled axons in the controls stopped at the edge of the lesion cavity, whereas (B) axons extended into the lesion site in contact with nanofibers (unmodified). The randomly folded nanofibrillar fabric (single arrows) can be detected due to its autofluorescence. Scale bar, 50 μm. (C) No labeling was detected when animals were sacrificed immediately after implantation of nanofibers, supporting the hypothesis that the axons observed represented regrowing axons, as opposed to axons spared in the lesion process. Scale bar, 50 μm.

microscopy. No axons were seen in the injury site in control animals (injury only, no nanofibers) (Fig. 4(A)), whereas they extended onto the nanofibrillar fabric (arrows), detectable in the injury site as a consequence of its low level of autofluorescence (Fig. 4(B)). No labeling was detected when animals were sacrificed immediately after implantation of nanofibers, indicating that the observed axons represented regrowth, as opposed to axons spared in the lesion process (Fig. 4(C)).

Covalent modification of the nanofibers with an extended version of the D5 peptide, called the D5′ peptide (amino acid sequence ADEGVFDNFVLKIRDTKKQ), enhanced their ability to facilitate neuronal process extension *in vitro*[19] and *in vivo* (compare Figs 5(A) and (B)). (The D5′ peptide has four additional amino acids at its N-terminus to allow for better presentation of the FD/FV active site to neurons.[19]) However, despite this encouraging result, this initial method of introducing nanofibers into the damaged spinal cord has proven to be unsatisfactory. The fabric itself was randomly folded during implantation, and regenerating axons appeared to follow along with the surface contours of the random folds, with forward motion at times restricted (Figs 5(B) and (C)) On the other hand, when the folds in the nanofibrillar fabric by chance fell parallel to the spinal cord axis, axons also grew with a parallel organization. This is illustrated in Figs 6(A) and (B), which focus in on the nanofibrillar implant within the lesion site. Therefore, these results suggest a necessity for engineering a nanofibrillar device with an ordered structure to appropriately and reproducibly direct axonal growth.

DISCUSSION

This work explores the utility of polyamide nanofibers as implantable substrates for the regeneration of

Polym Int **56**:1340–1348 (2007)
DOI: 10.1002/pi

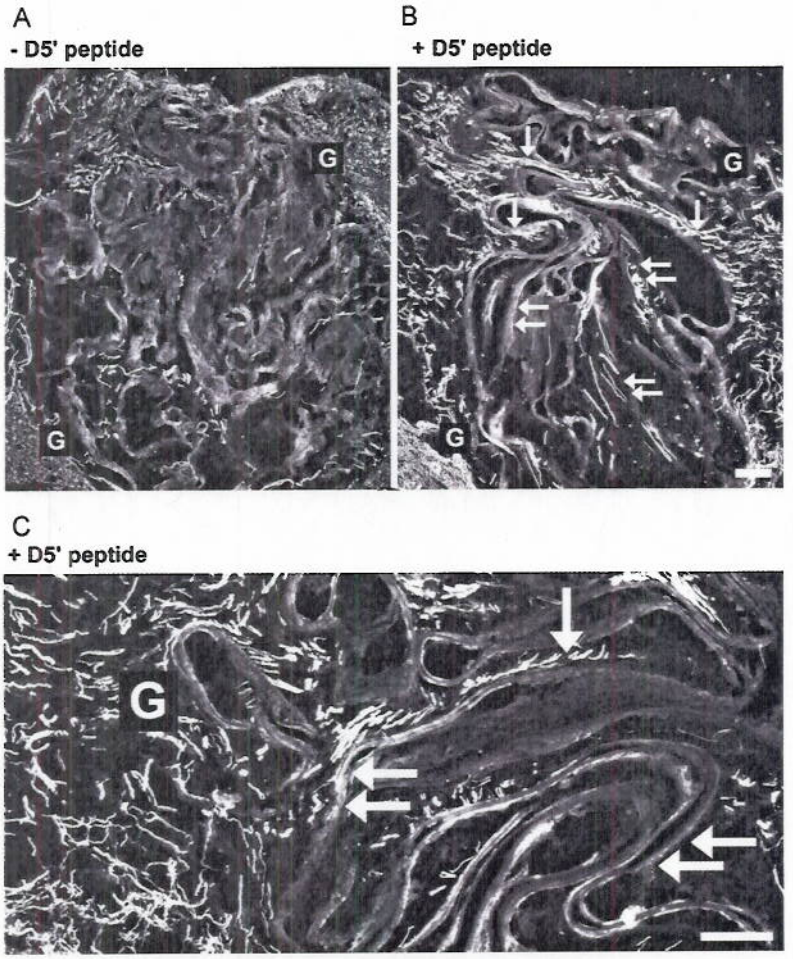

Figure 5. Peptide modification enhances the ability of nanofibers to promote axonal regrowth. Rostral is to the left. G, host–graft interface. Curves were adjusted in Adobe Photoshop for each panel to enhance the visibility of the axons against the autofluorescence of the nanofibers. (A) Neurofilament-M-labeled axons were observed within the implant of unmodified nanofibers. (B) Axonal growth was more robust within the implant of nanofibers modified with the D5′ peptide. Scale bar, 150 μm. (C) Axons were observed on the surface of the nanofibers following folds in the nanofibrillar fabric. The top of the image is *ca* 300 μm ventral to the top of the spinal cord. Scale bar, 300 μm. Single arrows in (B) and (C) denote axons growing more or less parallel to the axis of the spinal cord. Double arrows denote axons that deviated from a parallel path.

axons in the lesioned spinal cord. Significantly, the polyamide composition of the nanofibers (proprietary, Donaldson Company, Inc., Minneapolis, MN) is not rapidly degradable *in vivo* (S. Meiners, personal observation) and has no apparent neurotoxicity,[19] and the nanofibers maintain their structural integrity *in vivo* for several weeks. It seems likely that the formation and then maintenance of the reformed neuronal circuitry within the spine might be best facilitated and maintained by scaffolds that only slowly degrade within the body. Moreover, breakdown of rapidly biodegradable materials such as polyglycolate or polylactate can result in the release of monomers (e.g. lactate) that can significantly lower the local pH[24] and negatively impact the viability of regenerating neurons. In addition, a recent study has highlighted the utility of non- or slowly degrading materials in general, and polyamide in particular, in the promotion of axonal regrowth in the peripheral nervous system (PNS).[25] Third, thin layers of polyamide nonwoven fabrics are extremely flexible,[26] allowing for excellent incorporation into the damaged spinal cord.

Because of the problems encountered with randomly folded polyamide nanofiber implants illustrated above, the nanofibrillar fabric is instead envisioned fashioned into a multilayered tubular construct, reminiscent of the bilayered tubular construct fabricated by Kidoaki *et al.*[9] as a prototype scaffold for implantation into arteries. A view of one type of multilayered polyamide nanofibers (engineered by Donaldson Co., Inc., using proprietary technology) which could potentially be employed is shown in Fig. 6(C). In this example, each layer (*ca* 0.5 μm thick) was separated by about 10 μm from the next. However, nanofibrillar layers will need to be designed that are separated by 50–200 μm to allow more room for cellular growth.[27,28] Moreover, parameters can be adjusted to yield a device with desired mechanical properties.

For experimental testing, the tubular construct will ideally be implanted into a completely transected

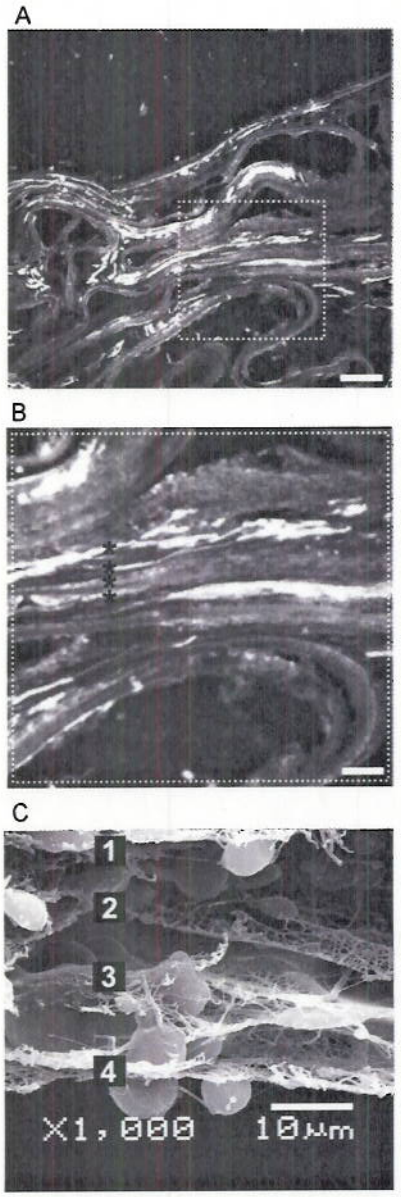

Figure 6. Orientation of the nanofibrillar fabric layers guides axonal regrowth. Rostral is to the left. Curves were adjusted in Adobe Photoshop for each panel to enhance the visibility of the axons against the autofluorescence of the nanofibers. (A) A view of axons growing on an implant of nanofibers modified with the D5′ peptide. The axons grew with a parallel organization when the nanofibrillar layers fell into a parallel array. Scale bar, 175 μm. (B) An enlarged view of axons shown in (A) demonstrating their parallel orientation (asterisks). Scale bar, 60 μm. (C) Multilayered nanofibers separated by spacers. These nanofiber layers incorporate only random nanofibers.

or near-completely transected spinal cord instead of the more modest over-hemisected spinal cord used in our studies, since very little sparing in the lateral corticospinal tract can lead to large effects on spared locomotion.[29] This can in turn lead to difficulty in behavioral testing to assess the effectiveness of the implant in promoting functional recovery. If nanofibers are to be used in actual human medicine, layers of nanofibers are envisioned as cut

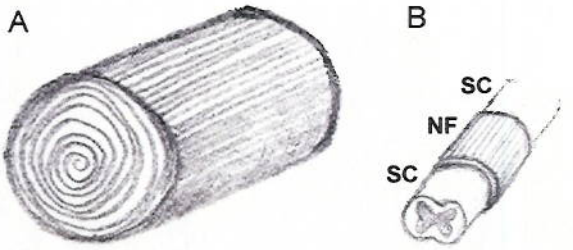

Figure 7. Schematic diagram of multilayered nanofibrillar implants. Implants grafted into the transected spinal cord with the longitudinal orientation of the layers parallel to the axis of the spinal cord. SC, spinal cord; NF, nanofibrillar implant.

and stacked to fit the size of the injury following, if necessary, trimming away of the scar tissue, which impedes axonal elongation. In the experimental model, the diameter of the multilayered tube will need to be fashioned to match the diameter of the transected spinal cord with the orientation of the layers parallel to the spinal cord axis (Fig. 7), allowing for longitudinally oriented axon growth. However, since neurite extension on randomly deposited nanofibers is itself random,[8,19] this design is not likely to limit lateral or dorsal-ventral axonal growth.

To overcome this problem, the nanofibrillar fabric should incorporate parallel, aligned nanofibers. Aligned nanofibers provide contact guidance cues to growing neurites, with neurite outgrowth exactly parallel to the nanofiber axis.[8] Thus aligned nanofibers will potentially allow directed growth from one end of the lesion to the other. However, a possible disadvantage of aligned nanofibers for tissue engineering in the spinal cord is their considerable rigidity in comparison to randomly deposited nanofibers,[30] with the potential to cause further trauma during implantation. Therefore, an aligned nanofibrillar fabric is pictured that consists of a very thin layer of nanofibers (*ca* 1 nanofiber thick) deposited in an aligned array on either side of a core of randomly deposited nanofibers. The aligned nanofibers should ideally be spaced *ca* 0.5–1 μm apart to maintain porosity. When formed into a multilayered tube and implanted such that the aligned fibers are parallel to the spinal cord, this nanofiber fabric will restrict longitudinal, lateral and dorsal-ventral growth of axons, while still retaining flexibility.

OTHER CONSIDERATIONS

Of course, further experiments are required to test the hypothesis that polyamide nanofibers or nanofibers of other compositions will be superior materials for spinal cord repair. For example, tract tracing studies must be done to evaluate whether axons in fact leave the implant, a necessity for the formation of functional connections. Furthermore, one must consider the inflammatory response and the scarring response. Injury to the CNS triggers an inflammatory reaction with potentially devastating

consequences. These include the production of pro-inflammatory cytokines by recruited inflammatory cells and activated endogenous CNS cells,[31–33] formation of a glial/fibrotic scar that impedes axonal regeneration,[34–36] axon dieback,[37] death of neurons and oligodendrocytes and production of inhibitory myelin products[38,39] and formation of cystic cavities.[40] Many biomaterials provoke a considerable foreign body response, with heightened inflammation and encapsulation of the implant by scar tissue[41] and ultimate rejection of the implant. As such, these biomaterials are unsuitable for tissue engineering.

However, polyamide nanofibers do not appear to provoke a considerable tissue response in the spinal cord as evidenced by low levels of scarring three and five weeks after injury in comparison to injury-only controls. Early experiments suggest that they are associated with reduced levels of glial fibrillary acidic protein, a marker for reactive astrocytes, and chondroitin sulfate proteoglycans, a group of molecules expressed by both glial and fibroblastic components of the scar and largely believed to be inhibitory to axonal regrowth[34,36] (not shown). Why this should be the case is at this point unclear. Attenuation of scarring may be due to the nanofibrillar nanostructure and porosity, which closely resemble features of naturally occurring extracellular matrix/basement membrane scaffolds and may therefore cause the nanofibers to look like 'self', or to the nanofibrillar chemistry, or to both.

CONCLUSIONS

Electrospun nanofibers have recently demonstrated widespread application in tissue culture due to their biomimetic properties and their structural resemblance to the extracellular matrix. The success of nanofibers for the culture of cells has generated great enthusiasm for their potential use in tissue engineering and regenerative medicine. However, to date very few *in vivo* applications of nanofiber technology have in fact been demonstrated. It is becoming increasingly clear that nanofibers will have to be electrospun into specialized scaffolds and structures in order to allow tissue regeneration within the body under conditions that allow physiologically relevant tissue formation. This is most obvious in the spinal cord, where axons follow a strict topography, much of which needs to be recreated in order to permit reconnection of appropriate circuits and maximal functional recovery following injury. Such structures must also incorporate within their design the ability to be 'stealthy' and not elicit the foreign body response or recognition by the immune system.

ACKNOWLEDGEMENTS

This work is dedicated to the memories of Lynn Elizabeth Meiners and Roger Keith Meiners. This work was supported by National Institutes of Health grant R01 NS40394 and New Jersey Commission on Spinal Cord Research grants 04-3034 SCR-E-O and 06A-007-SCR1 to SM. We thank Dr. Melvin Schindler (Nanoculture, LLC, Piscatway, NJ) for helpful discussions and critical reading of the manuscript. The polyamide nanofibers (Ultra-Web™) described in this work are available from Donaldson Co., Inc. (Minneapolis, MN, USA; http://www.donaldson.com/en/filtermedia/nanofibers/index.html or www.synthetic-ecm.com).

REFERENCES

1 Silver J and Miller JH, *Nat Rev Neurosci* **5**:146 (2004).
2 Chernousov MA and Carey DJ, *Histol Histopathol* **15**:593 (2000).
3 Adams JC and Tucker RP, *Dev Dyn* **218**:280 (2000).
4 Lein PJ, Banker GA and Higgins D, *Brain Res Dev Brain Res* **69**:191 (1992).
5 Kearns SM, Laywell ED, Kukekov VK and Steindler DA, *Exp Neurol* **182**:240 (2003).
6 Silver J, *J Neurol* **242**:S22–24 (2004).
7 Li W-J, Laurencin CT, Caterson EJ, Tuan RS and Ko FK, *J Biomed Mater Res A* **60**:613 (2002).
8 Yang F, Murugan R, Wang S and Ramakrishna S, *Biomaterials* **26**:2603 (2005).
9 Kidoaki S, Kwon IK and Matsuda T, *Biomaterials* **26**:37 (2005).
10 Ma Z, He W, Yong T and Ramakrishna S, *Tissue Eng* **11**:1149 (2005).
11 Venugopal J and Ramakrishna S, *Appl Biochem Biotechnol* **125**:147 (2005).
12 Schindler M, Nur-E-Kamal A, Ahmed I, Kamal J, Liu H-Y, Amor N, *et al*, *Cell Biochem Biophys* **45**:215 (2006).
13 Kim K-H, Jeong L, Park H-N, Shin S-Y, Park W-H, Lee S-C, *et al*, *J Biotechnol* **120**:327 (2005).
14 Gotz B, Scholze A, Clement A, Joester A, Schutte K, Wigger F, *et al*, *J Cell Biol* **132**:681 (1996).
15 Dorries U, Taylor J, Xioa Z, Lochter A, Montag D and Schachner M, *J Neurosci Res* **43**:420 (1996).
16 Meiners S and Geller HM, *Mol Cell Neurosci* **10**:100 (1997).
17 Meiners S and Mercado MLT, *Molec Neurobiol* **27**:177 (2003).
18 Meiners S, Nur-e-Kamal MSA and Mercado MLT, *J Neurosci* **21**:7215 (2001).
19 Ahmed I, Liu H-Y, Mamiya PC, Ponery AS, Babu AN, Weik T, *et al*, *J Biomed Mater Res A* **76**:851 (2006).
20 Schindler M, Ahmed I, Kamal J, Nur-e-Kamal A, Grafe TH, Chung HY, *et al*, *Biomaterials* **26**:5624 (2005).
21 Wiesendanger R, *Scanning Probe Microscopy and Spectroscopy: Methods and Applications*. Cambridge University Press, Cambridge, UK, Sections 2.4 and 2.5 (1994, reprinted 1998).
22 Braga PC and Ricci D, *Atomic Force Microscopy: Biomedical Methods and Applications (Methods in Molecular Biology)*. Humana Press, Totowa, NJ (2004).
23 Karakecili A, Satriano C, Gumusderelioglu M and Marletta G, *J Mater Sci: Mater Med* **18**:317 (2007).
24 Cordewener FW, van Geffen MF, Joziasse CAPSJP, Bos RRM, Rozema FR and Pennings AJ, *Biomaterials* **21**:2433 (2000).
25 Yannas IV and Hill BJ, *Biomaterials* **25**:1593 (2004).
26 Moeschel K, Nouaimi M, Steinbrenner C and Bisswanger H, *Biotech Bioeng* **82**:190 (2002).
27 Stokols S and Tuszynski MH, *Biomaterials* **25**:5839 (2004).
28 Yu TT and Shoichet MS, *Biomaterials* **26**:1507 (2005).
29 Keyvan-Fouladi N, Raisman G and Li Y, *J Neurosci* **23**:9428 (2003).
30 Lee CH, Shin HJ, Cho IH, Kang Y-M, Kim IA, Park K-D, *et al*, *Biomaterials* **26**:1261 (2005).
31 Giulian D, Chen J, Ingeman JE, George JK and Noponen M, *J Neurosci* **9**:4416 (1989).
32 Yang L, Blumbergs PC, Jones NR, Manavis J, Sarvestani GT and Ghabriel MN, *Spine* **29**:966 (2004).

33 Okada S, Nakamura M, Mikami Y, Shimazaki T, Mihara M, Ohsugi Y, *et al*, *J Neurosci Res* **76**:65 (2004).
34 McKeon RJ, Schreiber RC, Rudge JS and Silver J, *J Neurosci* **11**:3398 (1991).
35 Liesi P and Kauppila T, *Exp Neurol* **173**:31 (2002).
36 Tang X, Davies JE and Davies SJ, *J Neurosci Res* **71**:427 (2003).
37 Kerschensteiner M, Schwab ME, Lichtman JW and Misgeld T, *Nat Med* **11**:572 (2005).
38 Beattie MS, *Trends Mol Med* **10**:580 (2004).
39 Gomes-Leal A, Corkill DJ, Freire MA, Picanco-Diniz CW and Perry VH, *Exp Neurol* **190**:456 (2004).
40 Fitch MT and Silver J, in *CNS Regeneration: Basic Sciences and Clinical Advances*, ed. by Tuszynski MH and Kordower JH. Academic Press, San Diego, CA, pp. 55–88 (1999).
41 Anderson JM and Shive MS, *Adv Drug Deliv Rev* **28**:5 (1997).

Polym Int **56**:1340–1348 (2007)
DOI: 10.1002/pi